

Tidal modulation of the gravity-wave momentum flux in the Antarctic mesosphere

P. J. Espy and G. O. L. Jones

British Antarctic Survey, Cambridge, UK

G. R. Swenson and J. Tang

University of Illinois, Urbana, Illinois, USA

M. J. Taylor

Utah State University, Logan, Utah, USA

Received 2 February 2004; revised 23 April 2004; accepted 13 May 2004; published 12 June 2004.

[1] Airglow imager and dynasonde/IDI radar wind measurements at Halley Station, Antarctica (76°S , 27°W) have been used to estimate the diurnal variation of the vertical fluxes of horizontal momentum carried by high-frequency atmospheric gravity waves. The cross-correlation coefficients between the vertical and horizontal wind perturbations were calculated from the sodium airglow imager data collected during four consecutive nights of near total darkness during July of 2000. These were combined with wind-velocity variances from coincident radar measurements to estimate the upper limit of the vertical flux of horizontal momentum during three-hour intervals throughout the period. The resulting momentum flux showed a marked semi-diurnal oscillation in the zonal and meridional components. Calculations of the momentum flux through the Na airglow show variations in period and phase consistent with the observations, implying that tidal propagation and modulated gravity-wave forcing may both affect observed wind variations. **INDEX TERMS:** 3332 Meteorology and Atmospheric Dynamics: Mesospheric dynamics; 3334 Meteorology and Atmospheric Dynamics: Middle atmosphere dynamics (0341, 0342); 3384 Meteorology and Atmospheric Dynamics: Waves and tides. **Citation:** Espy, P. J., G. O. L. Jones, G. R. Swenson, J. Tang, and M. J. Taylor (2004), Tidal modulation of the gravity-wave momentum flux in the Antarctic mesosphere, *Geophys. Res. Lett.*, *31*, L11111, doi:10.1029/2004GL019624.

1. Introduction

[2] Upward-propagating atmospheric tides, driven by the absorption of solar radiation in the troposphere and stratosphere, and atmospheric gravity waves play important roles in the dynamics and thermal balance of the mesosphere [Forbes, 1984]. There have been extensive studies from ground and space of the diurnal tide (24-hour period), dominating in the sub-tropics, and the semi-diurnal tide (12-hour period), prominent at high latitudes [Forbes, 1984]. A ubiquitous feature of the observations is the large day-to-day variability of the amplitudes of the diurnal and semi-diurnal mesospheric wind components [Manson *et al.*, 1982; Hall *et al.*, 1995; Burrage *et al.*, 1995].

[3] Walterscheid [1981] suggested the tidal winds represent an oscillating mean to the gravity waves that modulate the mean-flow acceleration at the imposed frequency to create this tidal variability. Since then, diurnal oscillations in the gravity-wave momentum flux [Fritts and Vincent, 1987] and the gravity-wave variance [Thayaparan *et al.*, 1995] have been observed using mid-latitude radars. In addition, applying the model developed by Fritts and Vincent [1987], Isler and Fritts [1996] and Nakamura *et al.* [1997] used low-latitude radar observations of variations in the diurnal tidal amplitudes and phases to infer gravity-wave interactions. To date, most observations have utilized radar measurements at low and mid latitudes, and have involved only the diurnal tide.

[4] In this paper, we present high-latitude, optical-imaging measurements to provide an independent measure of the cross-correlation between the vertical and horizontal wind perturbations caused by gravity waves. These are combined with radar wind observations to infer the vertical flux of horizontal momentum. It is found that both the correlation coefficients and the observed and calculated momentum fluxes exhibit a strong semi-diurnal oscillation that is not in phase with the local tidal winds.

2. Instrumentation and Observations

[5] As part of a collaboration between Utah State University (USU) and the British Antarctic Survey (BAS), observations of the sodium (Na) night airglow were made using a monochromatic imaging system developed by USU to observe gravity-wave induced intensity fluctuations. The camera consisted of a cooled (-45°C), bare, 512×512 (effective) charge coupled device (CCD) array. This was coupled to a fast, $f/4$, telecentric lens system to produce an all-sky image. A 2 nm band-pass filter centred at 589 nm was used to isolate the Na emission. Each image was integrated on the CCD for 90 s before being digitized to 16 bits, and the image repetition rate was ~ 6 min. With the high sensitivity of the camera system, gravity-wave perturbations of the Na airglow intensity of a few percent were readily observed. Waves observed by such systems are characterized by vertical wavelengths greater than 12 km, short horizontal wavelengths ($\lambda < 150$ km) and large phase speeds ($C_1 > 40$ m/s) [Swenson and Gardner, 1998].

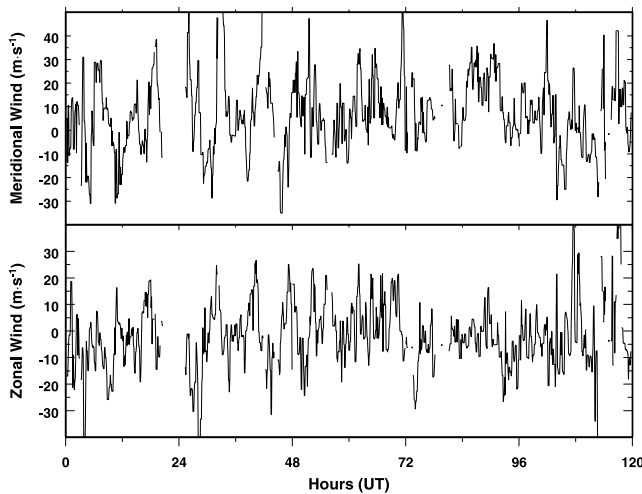


Figure 1. The IDI observed zonal (bottom) and meridional (top) winds at 90 km for the period 1–5 July 2000.

[6] The radar at Halley is a digital ionospheric sounder, or dynasonde, that has been run as an Imaging Doppler Interferometer (IDI) since 1996 [Jones *et al.*, 1997; Charles and Jones, 1999]. Operating at 2.75 MHz with a pulse length of 48 μ s, soundings are made for 102 s and repeated every 5 min. The echo returns are sorted by height into 5 km bins between 50 and 105 km, although most of the IDI echoes are obtained above 80 km. The location and line-of-sight velocity of each echo observed in a given height bin are used to fit a 3-D vector wind for that bin, allowing tidal variations and gravity-wave fluctuations to be monitored. The precision of the wind estimates are determined by the number of echoes observed, generally lying in the range of ± 4 m/s [Jones *et al.*, 1997].

[7] The observations were carried out at Halley, Antarctica over a 4-night period from 1–5 July 2000 that was characterized by clear weather. The IDI winds at 90 km for the period are shown in Figure 1. The daily averaged Kp values during this period ranged between 1+ and 2, so that there was little auroral contamination of either the images or the radar data. Due to the polar night, 15 hours of continuous optical observations were possible each day, and the radar operated with only minor maintenance stoppages.

3. Analysis and Results

[8] The all-sky Na image sequence over each 3-hour period was analyzed for spectral content using the procedure described in Gardner *et al.* [1996]. Briefly, the three-dimensional Fourier spectrum in frequency and the horizontal wavenumbers was computed for each image sequence. The unambiguous two-dimensional horizontal wavenumber spectrum, describing the distribution of gravity-wave energy as a function of horizontal scale and propagation direction, was computed by integrating over frequency. This included the effects of waves with observed periods between 12 minutes (the temporal Nyquist limit) and 2 hours, and horizontal wavelengths between 2.4 km (the spatial Nyquist limit) and 150 km. The unambiguous two-dimensional spectrum was then integrated over this wavenumber range to create an angular spectrum represent-

ing the azimuthal distribution of relative Na intensity variance.

[9] Gardner *et al.* [1999] has shown that the cross-correlation coefficients between the vertical and horizontal winds, which are the momentum fluxes normalized by the respective RMS wind perturbations, can be expressed as a simple integral over this azimuthal distribution of intensity variance as:

$$\langle w' \begin{pmatrix} u' \\ v' \end{pmatrix} \rangle = \frac{G \cdot \int_0^{2\pi} d\phi \frac{\langle I'_{Na}(\phi)^2 \rangle}{\bar{I}_{Na}^2} \begin{pmatrix} \sin(\phi) \\ \cos(\phi) \end{pmatrix}}{\left[\int_0^{2\pi} d\phi \frac{\langle I'_{Na}(\phi)^2 \rangle}{\bar{I}_{Na}^2} \cdot \int_0^{2\pi} d\phi \frac{\langle I'_{Na}(\phi)^2 \rangle}{\bar{I}_{Na}^2} \begin{pmatrix} \sin^2(\phi) \\ \cos^2(\phi) \end{pmatrix} \right]^{1/2}} \quad (1)$$

Where w'_{rms} , u'_{rms} and v'_{rms} are the RMS values of vertical and horizontal zonal and meridional wind perturbations, while \bar{I}_{Na} and I'_{Na} are the mean value and relative perturbation of the Na emission intensity caused by gravity waves moving in the azimuthal direction, ϕ . The vertical flux of horizontal momentum is directly proportional to these correlation coefficients scaled by the standard deviations of the horizontal and vertical winds derived from the radar data.

[10] The above relations and the factor, G , which sets the range of the cross-correlation coefficients, were developed using the gravity-wave polarization relations and employing a canonical power-law model for the frequency distribution of horizontal velocity variance. As a model frequency spectrum (spectral slope = 2) is integrated from the inertial to the Brunt frequency, it is not necessary to compensate for the Doppler effects associated with the mean background wind. For the exact form of G and uncertainties of the zonal and meridional cross-correlation coefficients, the reader is referred to Gardner *et al.* [1999]. As the method assumes that all waves propagate upwards and are not ducted, it provides only an upper limit to the momentum flux. However, Gardner *et al.* [1999] validated the momentum fluxes using this method with those measured by a Na wind lidar.

[11] To employ this procedure, the images were flat-fielded to remove van Rhijn effect, and stars removed using the technique described by Tang *et al.* [2003]. The center 150 km square field of view was interpolated to a 256 grid, and the unambiguous two-dimensional Fourier spectrum of the airglow perturbations calculated for each 3-hour image sequence. Three-hour intervals were a compromise to provide periods sufficiently long for estimating gravity-wave variations whilst affording an adequate sampling of tidal effects. The angular spectrum of the relative Na intensity variance was calculated by integrating this unambiguous Fourier spectrum over wavenumber. The zonal and meridional components of the correlation coefficients between the horizontal and vertical winds were then calculated from this angular spectrum as described above.

[12] Figure 2 shows the correlation coefficients calculated in this way over the 4-night period. The meridional and zonal coefficients are generally northward (positive) and westward (negative), respectively. This is consistent with gravity waves being filtered by an underlying wintertime circulation of southward (pole-ward) and eastward winds

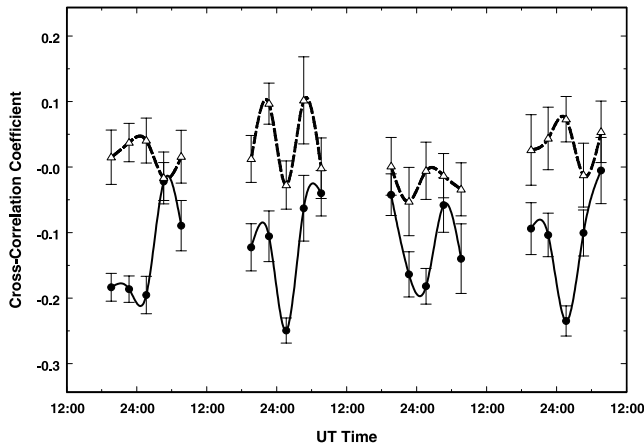


Figure 2. The 3-hourly zonal (solid circles) and meridional (open triangles) cross-correlation coefficients between the horizontal and vertical wind perturbations, calculated using the spectral content of the Na airglow images, are shown over the 4-night observation period along with a spline curve. A clear semi-diurnal oscillation is present in both components.

[Garcia and Solomon, 1985]. The smaller meridional coefficients compared to the zonal shows that the relatively weak meridional circulation is less effective at creating asymmetry in the gravity-wave field through filtering than the strong zonal circulation. Similarly, there are apparent tidal oscillations present in both components of the correlation coefficients, with the zonal amplitude larger. A Lomb-Scargle periodogram confirmed the presence of 8, 12 and 24-hour oscillations, with the semi-diurnal oscillation dominant and only statistically significant in the zonal component at the 92% confidence level.

[13] The radar winds over the 4-night period were processed, and the standard deviations of the horizontal and vertical components were computed for the same 3-hour intervals to scale the correlation coefficients to momentum flux. As two intervals were not covered by wind measurements, we performed a superposed-epoch analysis over the four nights to examine the tidal behavior of both the correlation coefficients and the momentum fluxes. Intervals for which wind variances were not available were excluded from the momentum-flux average. Figure 3 shows the average daily behavior of the zonal and meridional correlation coefficients and momentum flux. Both may be seen to have the same semi-diurnal variation and phase shift between the components, indicating that the radar-wind variances do not significantly alter the tidal modulation seen in the imager-derived correlation coefficients.

[14] To test if model tidal winds could reproduce the observed gravity-wave modulation, the flux of saturated gravity waves was evaluated using [Holton, 1983]:

$$u'w' = -\frac{\gamma k(\bar{u} - c)^3}{2N}. \quad (2)$$

The factor, $\gamma \cdot k$, is a scaling used in global models to reproduce the observed wind and temperature fields [Garcia and Solomon, 1985]. The physical interpretation is that γ is an “efficiency” factor (≤ 1) to account for the probability that

waves will not be present at all times [Holton, 1983]. The characteristic gravity-wave horizontal wavenumber, k , is assumed to be constant for all waves in the distribution [Holton, 1983], and their phase speeds are given by c . The Brunt-Väisälä frequency, N , and the mean horizontal wind, \bar{u} , are evaluated at the altitude for which the flux is to be calculated. This expression was used to estimate the saturated gravity-wave momentum flux at the Na emission altitude assuming an initial phase-speed distribution near 10 km that was constant between ± 70 m/s for waves that would saturate above 60 km [Alexander and Rosenlof, 1996]. To account for gravity waves ceasing to propagate beyond heights where their phase velocity matched the mean wind velocity, the Horizontal Neutral Wind Model (HWM-93) [Hedin et al., 1996] was processed for the data intervals to eliminate those waves from the distribution reaching 90 km. The momentum flux in each 3-hour bin was then calculated integrating Equation 2 over this distribution and the HWM-93 winds at 90 km. Under the assumption of a constant spectrum, the calculated saturated wave behavior was taken as a tracer of the entire wave distribution observed by the imager.

[15] The resulting zonal and meridional components, least-squares fitted to the data using the same scaling, $\gamma \cdot k$, are shown in Figure 4 along with the observed horizontal momentum flux. The calculated flux reproduces the relative levels of observed zonal and meridional fluxes. Additionally, the tidal filtering reproduces both the observed modulation and the phase shift between the components.

4. Discussion and Conclusions

[16] Interactions between tidal and gravity waves might play a large role in the observed short-term variability of the high-latitude semi-diurnal tide [Charles and Jones, 1999]. To examine this, we have used high-latitude,

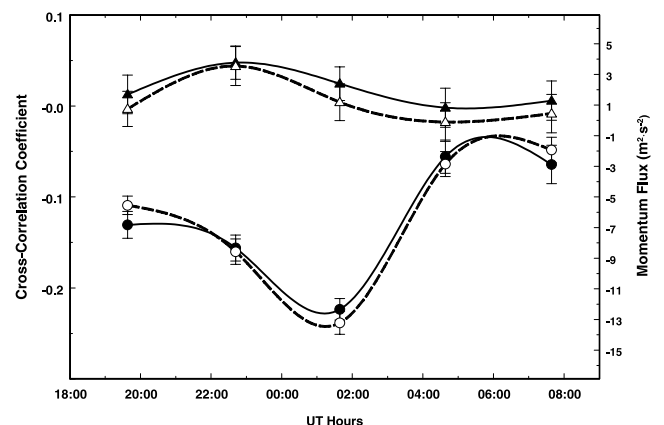


Figure 3. The superposed epoch values of the zonal (solid circles) and meridional (solid triangles) cross-correlation coefficients between the horizontal and vertical wind perturbations are shown with solid spline curves. The upward flux of horizontal momentum in the zonal (open circles) and meridional (open triangles) carried by gravity waves are shown with broken spline curves and referenced to the right hand axis. There is an excellent correspondence between the two, and both display a semi-diurnal oscillation with the zonal component leading the meridional by ~ 3 hours.

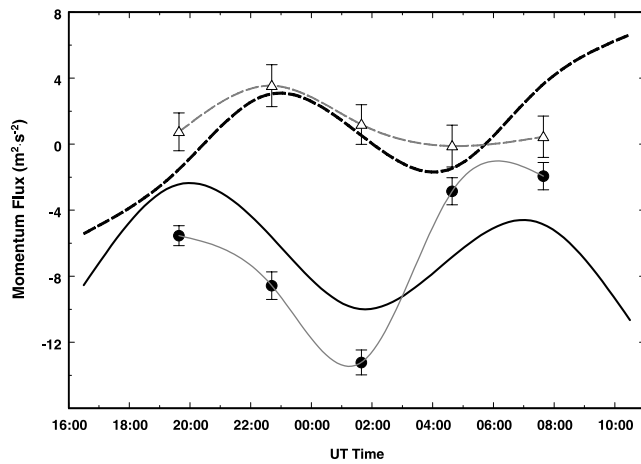


Figure 4. The superposed epoch values of the zonal (solid circles/light-solid spline) and meridional (open triangles/light-dashed spline) upward flux of horizontal momentum carried by gravity waves are shown. The gravity-wave momentum deposited at the altitude of the Na airglow emission, calculated using Equation 2 and the HWM-93 model winds, is shown for the zonal (solid line) and meridional (dashed line) directions.

optical-imaging measurements to provide an independent measure of the cross-correlation between the vertical and horizontal wind perturbations caused by gravity waves. Combining this with wind variances from co-located radar measurements, the zonal and meridional components of the vertical flux of horizontal momentum through the Na airglow region were obtained. Both the correlation coefficients and the momentum fluxes display a marked semi-diurnal oscillation. Although the zonal modulation is larger, there is evidence of meridional interactions as well. As with the diurnal tide [Fritts and Vincent, 1987; Thayaparan et al., 1995], the sense of this variation is out of phase with the local semi-diurnal tidal winds.

[17] Given the observation of interactions between the diurnal tide and gravity waves at low and mid latitudes [Fritts and Vincent, 1987; Thayaparan et al., 1995; Isler and Fritts, 1996; Nakamura et al., 1997], it is not surprising to see the gravity-wave momentum flux modulated by the semi-diurnal tide at the high latitudes where it dominates. Our interpretation of tidal modulation of the gravity-wave momentum is strengthened through a straightforward calculation of gravity-wave transmission and momentum flux. This displays not only the same semi-diurnal variation as the measured momentum flux, but also matches the phase and relative magnitudes of the zonal and meridional components. This modulated gravity-wave momentum flux through the Na layer can accelerate overlying winds with this imposed variability, influencing the semi-diurnal tidal amplitudes and phases inferred from these winds [Walterscheid, 1981].

[18] In conclusion, the observational results presented here show that the upward momentum carried by gravity waves is modulated by the semi-diurnal tide at high-latitudes. The modulated gravity-wave momentum will contribute significantly to the observed variability of the high-latitude semi-diurnal tide. This study not only extends the latitude and tidal-mode coverage of gravity-wave interactions with the tide, it demonstrates that non-directional

radar measurements may be combined with optical imaging observations to provide a measure of the direct modulation of the gravity-wave momentum flux by tides.

[19] **Acknowledgment.** The Halley imager was jointly supported by US National Science Foundation grants ATM-0003180 and OPP-9816465, and by the UK Natural Environment Research Council.

References

- Alexander, M. J., and K. H. Rosenlof (1996), Non stationary gravity wave forcing of the stratospheric mean wind, *J. Geophys. Res.*, *101*(D18), 1571–1588.
- Burrage, M. D., M. E. Hagan, W. R. Skinner, D. L. Wu, and P. B. Hays (1995), Long-term variability in the solar diurnal tide observed by HRDI and simulated by the GSWM, *Geophys. Res. Lett.*, *22*(19), 2641–2644.
- Charles, K., and G. O. L. Jones (1999), Mesospheric mean winds and tides observed by the imaging Doppler interferometer (IDI) at Halley, Antarctica, *J. Atmos. Sol. Terr. Phys.*, *61*, 351–362.
- Forbes, J. M. (1984), Middle atmosphere tides, *J. Atmos. Terr. Phys.*, *46*, 1049–1067.
- Fritts, D. C., and R. A. Vincent (1987), Mesospheric momentum flux studies at Adelaide, Australia: Observations and a gravity wave-tidal interaction model, *J. Atmos. Sci.*, *44*, 605–619.
- Garcia, R. R., and S. Solomon (1985), The effect of breaking gravity waves on the dynamics and chemical composition of the mesosphere and lower thermosphere, *J. Geophys. Res.*, *90*, 3850–3868.
- Gardner, C. S., K. Gulati, Y. Zhao, and G. Swenson (1999), Measuring gravity wave momentum fluxes with airglow imagers, *J. Geophys. Res.*, *104*(D10), 1903–1915.
- Gardner, C. S., M. Coble, G. C. Papen, and G. R. Swenson (1996), Observations of the unambiguous 2-dimensional horizontal wave number spectrum of OH intensity perturbations, *Geophys. Res. Lett.*, *23*(25), 3739–3742.
- Hall, G. E., S. P. Nambathiri, A. H. Manson, and C. E. Meek (1995), Daily tidal, planetary wave, and gravity wave amplitudes over the Canadian prairies, *J. Atmos. Terr. Phys.*, *57*, 1553–1567.
- Hedin, A. E., E. L. Fleming, A. H. Manson, F. J. Schmidlin, S. K. Avery, R. R. Clark, S. J. Franke, G. J. Fraser, T. Tsuda, F. Vial, and R. A. Vincent (1996), Empirical wind model for the upper, middle and lower atmosphere, *J. Atmos. Terr. Phys.*, *58*, 1421–1447.
- Holton, J. R. (1983), The influence of gravity wave breaking on the general circulation of the middle atmosphere, *J. Atmos. Sci.*, *40*, 2497–2507.
- Isler, J. R., and D. C. Fritts (1996), Gravity wave variability and interaction with lower-frequency motions in the mesosphere and lower thermosphere over Hawaii, *J. Atmos. Sci.*, *53*, 37–48.
- Jones, G. O. L., K. Charles, and M. J. Jarvis (1997), First mesospheric observations using an imaging Doppler interferometer adaptation of the dynasonde at Halley, Antarctica, *Radio Sci.*, *32*(6), 2109–2122.
- Manson, A. H., C. E. Meek, J. B. Gregory, and D. K. Chakrabarty (1982), Fluctuations in tidal (24-h, 12-h) characteristics and oscillations (8-h-5-d) in the mesosphere and lower thermosphere 970–110 km): Saskatoon (52°N, 107°W), 1979–81, *Planet. Space Sci.*, *39*, 1283–1294.
- Nakamura, T., D. C. Fritts, J. R. Isler, T. Tsuda, R. A. Vincent, and I. M. Reid (1997), Short-period fluctuations of the diurnal tide observed with low-latitude MF and meteor radars during CADRE: Evidence for gravity wave/tidal interactions, *J. Geophys. Res.*, *102*(D22), 26,225–26,238.
- Swenson, G. R., and C. S. Gardner (1998), Analytical models for the responses of the mesospheric OH* and Na layers to atmospheric gravity waves, *J. Geophys. Res.*, *103*(D6), 6271–6294.
- Tang, J., F. Kamalabadi, L. G. Rumsey, and G. R. Swenson (2003), Point source suppression for atmospheric wave extraction from airglow imaging measurements, *IEEE Trans. Geosci. and Remote Sens.*, *41*, 146–152.
- Thayaparan, T., W. K. Hocking, and J. MacDougall (1995), Observational evidence of tidal/gravity wave interactions using the UWO 2MHz radar, *Geophys. Res. Lett.*, *22*(4), 373–376.
- Walterscheid, R. L. (1981), Inertio-gravity wave induced accelerations of mean flow having an imposed periodic component: Implications for tidal observations in the meteor region, *J. Geophys. Res.*, *86*, 9698–9706.

P. J. Espy and G. O. L. Jones, The British Antarctic Survey, Physical Sciences Division, High Cross, Madingley Road, Cambridge, CB3 0ET, UK. (pje@bas.ac.uk)

G. R. Swenson and J. Tang, Department of Electrical and Computer Engineering, University of Illinois at Urbana-Champaign, 313 CSRL, 1308 West Main Street, Urbana, IL 61801, USA.

M. J. Taylor, Department of Physics, Utah State University, Logan, UT 84322, USA.